Thesis for the Degree of Master of Science

Color Variability of HBC 722 in the Post-Outburst Phases

Giseon Baek

School of Space Research

Graduate School

Kyung Hee University

Seoul, Korea

August, 2014

Color Variability of HBC 722 in the Post-Outburst Phases

Giseon Baek

School of Space Research

Graduate School

Kyung Hee University

Seoul, Korea

August, 2014

Color Variability of HBC 722 in the Post-Outburst Phases

by

Giseon Baek

Advised by

Dr. Sami Khan Solanki

Submitted to the School of Space Research
and the Faculty of the Graduate School of
Kyung Hee University in partial fulfillment
of the requirements for the degree of
Master of Science

Dissertation Committee:

Prof. Sungsoo S. Kim (Chairman), Ph.D.....................

Prof. Sami Khan Solanki, Ph.D..............................

Prof. Soojong Pak, Ph.D....................................

Color Variability of HBC 722 in the Post-Outburst Phase[1]

by

Giseon Baek

Submitted to the School of Space Research
on June 30, 2014, in partial fulfillment of the
requirements for the degree of
Master of Science

Abstract

We carried out photometric observations for HBC 722 in SDSS r, i and z bands from 2011 April to 2013 May with a Camera for Quasars in Early uNiverse attached to the 2.1m Otto Struve telescope at McDonald Observatory. The post-outburst phenomena are classified into five phases according to not only brightness but also color variations, which might be caused by physical changes in the emitting regions of optical and near-infrared bands. A series of spectral energy distribution (SED) is presented to support color variations and track the time evolution of SED in optical/near-infrared region after the outburst. We also examined short term variability (intra-day and day scale) to find evidences of flickering by using the micro-variability method. We found clear signs of day scale variability and weak indications of intra-day scale fluctuations, which implies that the flickering event occurs in HBC 722 after outburst.

Thesis Supervisor: Sami Khan Solanki
Title: Professor

[1]This work is submitted to Astronomical Journal on 2014 June 6 with the same title and contents as this thesis. The authors of the submitted manuscript are Giseon Baek, Soojong Pak, Joel D. Green, Jeong−Eun Lee, Yiseul Jeon, Changsu Choi, Myungshin Im, Hyun−Il Sung, and Won−Kee Park.

국 문 초 록

우리는 2010년 9월 급작스럽게 가시광에서 5등급 가량의 폭발적인 변광을 일으킨 전주계열성 HBC 722에 대한 측광 관측을 수행하였다. 관측은 맥도널드 천문대 2.1m 망원경에 CQUEAN을 부착하여 SDSS *r, i, z* 밴드에서 2011년 4월부터 2013년 5월에 걸쳐 이루어졌다. 우리는 분석을 위해 HBC 722의 2010년 폭발적인 변광 이후를 천체의 밝기와 색 변화에 따라 5개의 시기로 분류하였는데, 이것은 천체가 가시광과 근적외선을 방사하는 지역에서의 물리적 변화에 기인했을 것으로 추정된다. 우리는 또한 가시광과 근적외선 영역에서의 스펙트럼 에너지분포를 나타내어 2010년의 폭발적인 변광 이후 나타난 천체의 색 변화를 설명하고 시간에 대한 스펙트럼 에너지분포를 확인하였다. 마지막으로 우리는 수 년에 이르는 긴 시간단위 변광과 구별되는 수 일 혹은 하루 미만의 짧은 시간단위 변광을 미세변광 방법으로 정량화하여 찾아내고자 하였다. 이 과정에서 뚜렷한 수 일 단위의 변광이 있음을 확인하였으며 하루 미만의 변광에 대한 단서를 얻었는데, 이것은 HBC 722가 폭발적인 변광을 일으킨 이후 시기에 flickering 현상을 나타냄을 암시하였다.

Contents

List of Figures

List of Tables

Chapter 1

Introduction

1.1 Introduction

FU Orionis type objects (FUors) are a group of pre-main sequence objects showing a long-lived outburst in optical bands (Hartmann & Kenyon 1996). A prototype of this group, FU Orionis, flared up by 6 magnitude in B band for a few months in 1936 and has stayed bright for ∼80 years and dimmed only 0.015 magnitude per year (Kenyon et al. 2000).

A dozen FUors have been discovered with analogous photometric features. They are located in an active star forming region, showing a rapid increase of optical brightness (3–5 mag) for a few months and a ring-shaped asymmetric reflection nebula appears after outburst (Goodrich 1987). They are expected to have decaying time of 10–100 years (Bell & Lin 1994) although there are small differences in each source (Hartmann & Kenyon 1996). Another dozen of FUors without an outburst have been found via spectral diagnosis. They have F–G supergiant spectum in optical, while K–M giant-supergiant spectrum in near-infrared wavelength region. In addition they show double-peaked line profiles, P Cygni profiles in Hα and infrared excess in spectral energy distribution (SED) (Weintraub et al. 1991; Lee et al. 2011)

FU Orionis type outburst phenomenon has been interpreted as a sudden increase in the accretion rate by a factor of 100–1000 in comparison to that in the quiescent state.

Throughout a whole outburst event, $\sim$0.01 $M_\odot$ of disk material is supplied to the central star (Bell & Lin 1994; Hartmann & Kenyon 1996). In this picture, material reaching to the innermost part of the circumstellar disk is dumped into the central star. This process in FUors might give rise to detectable sign of accretion and material dumping at inner edge of the disk, often dealt with "flickering". It can cause inhomogeneities (cool or hot spots) on stellar surface or disk instability, which is believed to be the reason of periodic or sporadic variabilities in hour – day timescale.

HBC 722 (also known as LkHα 188 G4, PTF 10qpf and V2493 Cyg) is located in the dark cloud region, named "Gulf of Mexico", in the southern part of the North America/Pelican Nebula Complex at a distance of 520 pc (Laugalys et al. 2006). HBC 722 is the second FUor with a well-characterized pre-outburst optical spectrum. Before outburst, the source had characteristics of classical T Tauri star with a mass of $\sim$ 0.5 $M_\odot$, bolometric luminosity of 0.85 $L_\odot$, visual extinction of 3.4 magnitude, and a small amount of variability generally seen in Class II young stellar object (YSO) (Semkov et al. 2010; Miller et al. 2011; Kóspál et al. 2011). Its prominent Hα features with equivalent width of 100 nm implies that the accretion activity is high even in the quiescent state (Cohen & Kuhi 1979).

In 2010 July, HBC 722 produced large amplitude optical outburst over a few months (ΔV= 4.7 mag), and was classified as FUors (Semkov et al. 2010; Miller et al. 2011). After the peak of 2010 September, it darkened by about 1.5 magnitude in V for 6 months unlike FUors. Kóspál et al. (2011) suggested that, with this rate of decline, HBC 722 could return to the quiescent state in a year. They claimed that it was necessary to reconsider the classification of the source as FUors, or as another category of flaring YSO with a shorter outburst duration period, like EXors. They also calculated some properties of HBC 722 after the outburst. They derived the accretion rate of 10^{-6} $M_\odot yr^{-1}$ and a bolometric luminosity of 8–12 $L_\odot$ assuming the mass of 0.5 $M_\odot$ and radius of 3 $R_\odot$. During the outburst, the luminosity rose roughly by a factor of 10 compared to the quiescence luminosity (0.85 $L_\odot$), which is somewhat smaller than classical FUors whose luminosity rises by a factor of 10–100, although the source often show typical spectra of FUors (Audard et al. 2014).

Since then, however, HBC 722 remained in a constant status with small fluctuations, maintaining the level brighter than quiescence by 3.3 magnitude (V) for a few months and then started to re-brighten (Semkov et al. 2012a; Green et al. 2013). We observed this re-brightened period in optical/near-infrared wavelengths to track the re-increase of the accretion rate of HBC 722. According to recent study, the source has gradually regained its brightness about 1.5 magnitude in V band over 2 years. Therefore, HBC 722 can be classified as FUors (Audard et al. 2014). Meanwhile, the color also has slightly changed during the re-brightened state. It became bluer by 0.2 magnitude in R-I color compared to the constant status (Semkov et al. 2014).

1.2 Thesis Outline

In this paper, we present the results of high cadence photometric observations from 2011 April to 2013 May. We traced variabilities of HBC 722 in multiple timescales (year, day and intra-day) and try to find evidence of flickering. In section 2, the details of observation strategies and data reduction techniques are described. We analyze behaviors of HBC 722 by using light curves, color curves, color-magnitude diagram and color-color diagram in section 3. In section 4, we discuss the time evolution of SEDs after outburst and diagnosis of flickering with day variability and intra-day variability (IDV) check. Finally, we summarize our conclusions in section 5. In this study, we use the AB magnitude system. Also, we deal with ‘long term’ as year- or longer timescale and ‘short term’ as day or intra-day timescale.

Chapter 2

Observations and Data reduction

2.1 Observations

We carried out photometric observations of HBC 722 using Camera for QUasars in EArly uNiverse (CQUEAN) attached to the 2.1 m Otto Struve telescope at the McDonald Observatory (Kim et al. 2011; Park et al. 2012). Using a 1024×1024 pixel deep-depletion CCD chip, CQUEAN has a 4.'7×4.'7 field of view with a custom-made focal reducer (Lim et al. 2013). We obtained minute scale cadence images in SDSS r, i and z bands in SDSS filter system (Fukugita et al. 1996) for 60 nights from 2011 April to 2013 May. To see the short scale behavior of HBC 722, we performed continuous time series monitoring observations for 2–8 hours in 18 nights. The observation field is shown in Green et al. (2013). The log of observations are listed in Table 1.

Table 1: Observing log

Date[a]	Time[a]	Julian Date	Exposure Time × Number of Frames[b]		
yyyy-mm-dd	hh:mm:dd	(+2450000)	r	i	z
2011-04-26	10:51:58	5677.9528	20×24	20×24	20×24
2011-04-30	10:59:49	5681.9582	15×30	15×30	15×30
2011-07-05	5:44:11	5747.7390	10×311	10×311	10×311
2011-07-06	8:23:28	5748.8496	10×5	10×5	10×5
2011-07-07	8:28:53	5749.8534	10×5	10×5	10×5
2011-07-08	8:20:31	5750.8476	10×5	10×5	10×5
2011-07-09	8:06:10	5751.8376	10×5	10×5	10×5
2011-07-11	7:32:59	5753.8146	10×47	10×47	10×47
2011-08-19	8:33:37	5792.8567	20×25	10×25	10×25
2011-08-21	6:24:41	5794.7671	20×15	10×15	10×15
2011-08-22	6:39:34	5795.7775	20×15	10×15	10×15
2011-08-23	4:38:42	5796.6935	20×15	10×15	10×15
2011-08-24	2:35:07	5797.6077	20×1125	···	···
2011-08-25	4:37:44	5798.6929	20×15	10×15	10×15
2011-08-26	5:12:55	5799.7173	20×12	10×12	10×12
2011-08-27	5:30:30	5800.7295	20×15	10×15	10×15
2011-08-28	4:55:42	5801.7054	20×15	10×15	10×15
2011-08-29	5:17:58	5802.7208	20×15	10×15	10×15
2011-08-30	5:14:34	5803.7185	20×10	10×10	10×10
2011-08-31	3:34:55	5804.6493	20×791	···	···
2011-09-01	6:19:49	5805.7638	30×14	15×2,10×12	10×14
2011-10-30	3:12:20	5864.6336	20×6	10×6	10×6
2011-10-31	2:29:53	5865.6041	20×15	10×15	10×15
2011-11-01	2:12:01	5866.5917	20×15	10×15	10×15
2011-11-02	1:05:49	5867.5457	20×12, 30×199	10×211	10×211

Date[a]	Time[a]	Julian Date	Exposure Time × Number of Frames[b]		
yyyy-mm-dd	hh:mm:dd	(+2450000)	*r*	*i*	*z*
2011-11-04	1:07:04	5869.5466	30×116	10×116	10×116
2011-11-05	2:14:58	5870.5937	30×14	10×14	10×14
2011-11-07	0:47:35	5872.5330	30×15	10×15	10×15
2011-11-08	1:31:37	5873.5636	30×3, 60×10	10×3, 20×10	10×3, 20×10
2011-11-09	0:48:21	5874.5336	30×179, 60×27	10×179, 20×27	10×179, 20×27
2011-12-14	2:09:20	5909.5898	90×3	30×3	30×3
2011-12-16	1:16:41	5911.5533	90×5	20×5	30×5
2012-05-27	8:28:31	6074.8531	20×45, 30×83	10×128	10×128
2012-05-30	7:24:56	6077.8090	15×300	4×300	4×300
2012-05-31	9:51:59	6078.9111	10×3	5×3	5×3
2012-06-26	7:54:30	6104.8295	15×30	4×30	4×30
2012-06-27	6:58:05	6105.7903	15×29	4×29	4×29
2012-06-28	5:09:22	6106.7148	15×222, 20×177	4×222, 6×177	4×222, 6×177
2012-06-29	5:43:15	6107.7384	15×30	4×30	4×30
2012-06-30	5:29:25	6108.7288	30×30	8×30	8×30
2012-07-01	7:10:07	6109.7987	30×182	8×182	8×182
2012-07-02	6:33:15	6110.7731	15×3, 30×29	4×3, 8×29	4×3, 8×29
2012-09-01	2:58:50	6171.6242	15×27, 20× 24, 30×277	4×328	4×328
2012-09-02	2:51:35	6172.6192	30×77, 10×259, 15×78, 20×78	4×414, 6×78	4×336, 6×156
2012-09-03	4:44:14	6173.6974	20×198, 30×21 5 ×48, 8×21	4×150, 8×3,10×18	5 ×150, 6×48,
2012-09-04	8:00:18	6174.8335	15×14	4×14	4×14
2012-09-05	7:14:20	6175.8016	10×38	4×38	5×38
2012-09-06	3:37:17	6176.6509	30×23	8×23	10×23
2012-09-07	2:35:53	6177.6083	10×31	4×31	6×31
2012-09-09	3:18:30	6179.6379	15×162, 30×15	4×162, 8×15	6×162, 12×15
2012-09-10	2:49:43	6180.6179	10×22	4×22	6×22

Date[a]	Time[a]	Julian Date	Exposure Time × Number of Frames[b]		
yyyy-mm-dd	hh:mm:dd	(+2450000)	r	i	z
2012-09-11	4:48:35	6181.7004	10×24	4×24	6×24
2012-09-12	6:07:20	6182.7551	30×5	8×5	12×5
2012-11-23	2:00:33	6254.5837	30×10	5×10	5×10
2012-11-24	1:52:13	6255.5779	20×30	5×30	5×30
2012-11-26	1:45:33	6257.5733	20×53	5×53	5×53
2013-04-30	9:03:50	6412.8777	15×162	4×162	4×162
2013-05-01	9:27:04	6413.8938	15×84, 10×60	4×144	4×144
2013-05-04	8:45:14	6416.8648	15×134, 30×9	4×134, 8×9	4×134, 10×9
2013-05-05	8:30:23	6417.8544	15×150	4×150	4×150

[a]Date and Time in UT. Time refers when observation started.

[b]Exposure time per frame in units of second.

Note. – r band data from 2011 April to 2012 July is mentioned in Green et al. (2013).

2.2 Data reduction

The images were reduced with the IRAF[1]/CCDRED packages. Since most of the images were exposed for less than 30 seconds, dark subtraction was unnecessary except for the 2011 December r band images. Aperture photometry was conducted by using Source Extractor (Bertin & Arnouts 1996). We set the aperture size with 3 times of FWHM of seeing of each night. Errors include Poisson errors, sky background fluctuations and subtraction errors for differential photometry. For the nightly averaged points, errors are denoted by standard deviation of comparison star in a night. Typical averaged error value is ≤ 0.01 magnitude.

Since HBC 722 is located in an active star forming region, most of the surrounding objects in our HBC 722 field are likely to be YSO, which could show small amplitude variabilities (Semkov et al. 2010; Green et al. 2013). Thus for the differential photometry, we had to carefully select comparison stars in the field. We carried out variability checks on the background objects by repetitive differential photometry paring two candidates. Finally C7 and C4 (see Table 2 for details) were chosen as a comparison star and check star respectively among 12 selections. We present spectral energy distributions of two objects in Figure 1. We take u and g bands data from Sloan Digital Sky Survey (SDSS) database and r, i and z bands data from this work. We also take magnitudes from Two Micron All Sky Survey (2MASS) point source catalog (Skrutskie et al. 2006) for J, H and Ks bands, and Wide-field Infrared Survey Explorer (WISE) source catalog for 3.4, 4.6 μm data (Wright et al. 2010). We converted magnitudes of 2MASS and WISE from Vega to AB magnitude system. In optical/near-infrared, both the comparison and the check star do not show any special features but have blackbody-like spectrum. We could fit

[1]IRAF is distributed by the National Optical Astronomy Observatory, which is operated by the Association of Universities for Research in Astronomy, Inc., under cooperative agreement with the National Science Foundation.

SEDs assuming a single temperature blackbody and obtained approximate temperature of 3400–3500 K (spectral type M2–M3) and 3500–3600 K (spectral type M3–M4) for C4 and C7, respectively.

Flux calibration was conducted using SDSS standard stars from Smith et al. (2002), taken in a photometric night during the 2012 June observing run. We considered the zero point and airmass terms of the standard calibration formula. However, secondary and higher order terms were small enough to be ignored in the flux calibration.

Table 2: Target list

Target	USNO-B1.0[a] ID	R.A. (2000)	Dec. (2000)	AB magnitude			Spectral Type
				r	i	z	
HBC 722	1338-0391463	20:58:17.0	+43:53:42.9	$14.3 \sim 12.5$[b]	$13.4 \sim 11.8$[b]	$12.8 \sim 11.2$[b]	late K–M[c]
C4[d]	1338-0391536	20:58:30.0	+43:52:23.8	14.31	13.80	13.50	M2–M3
C7	1338-0391522	20:58:26.3	+43:52:23.5	15.15	14.53	14.20	M3–M4

[a] http://www.nofs.navy.mil/data/fchpix/

[b] Brightness changes in our observed period (2011 April – 2013 May) are shown.

[c] Miller et al. (2011)

[d] Coordinate and r mag from Green et al. (2013) are quoted.

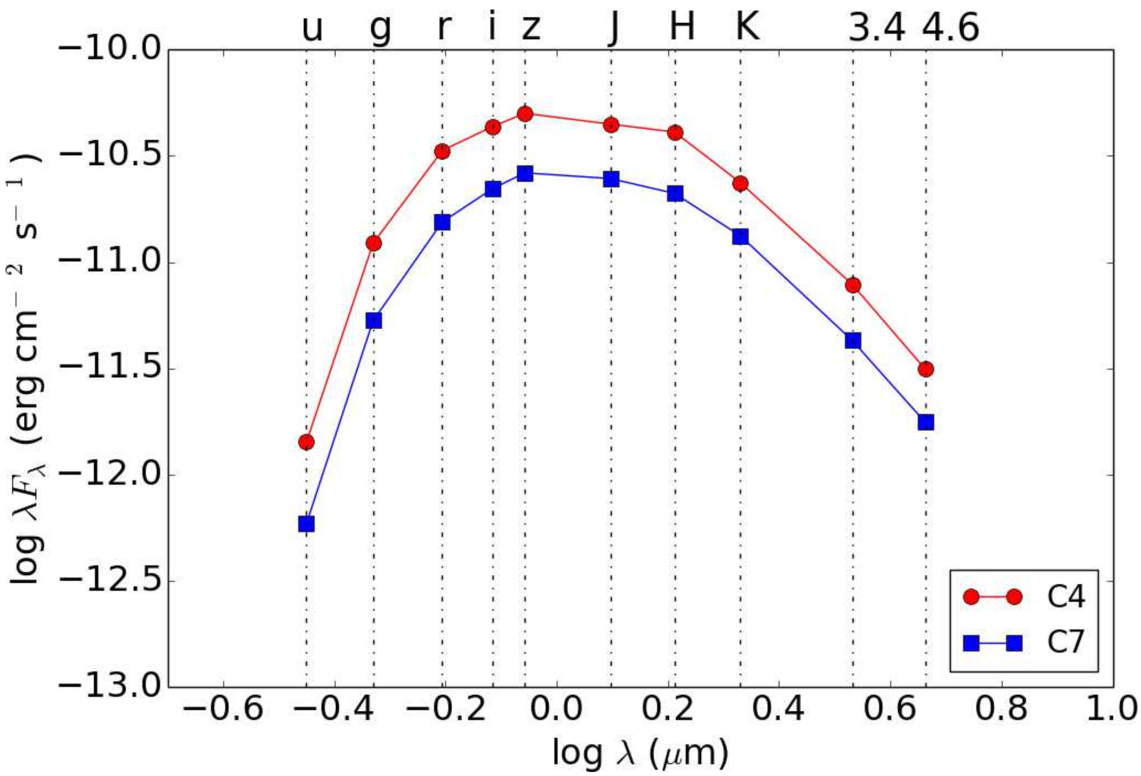

Fig. 1: Spectral energy distributions of comparison (C7) and check star (C4). In addition to r, i and z from this work, archival data from SDSS, 2MASS and WISE are adopted.

Chapter 3

Results

3.1 Monitoring brightness and color variabilities

We observed HBC 722 from 2011 April to 2013 May, during constant and re-brightened periods of the object. The upper part of Figure 2 shows light curves for our observations in r, i and z bands and Johnson-Cousins R and I band literature data for comparison (Semkov et al. 2012a,b, 2014). We converted the magnitudes of R and I bands from Vega to AB magnitude system using Blanton & Roweis (2007). Our observation and archival data are fairly consistent in terms of monotonic behaviors of brightness, though there are small offsets of magnitude due to differences in filter system. From 2011 April to 2013 May, r band brightened 1.8 mag and i and z bands brightened 1.6 magnitude including smaller scale variations. For comparison, R and I bands from Semkov et al. (2012a, 2014) got brighter by 1.73 and 1.55 magnitude in the same period. The bottom part of Figure 2 presents long term color curves. At the same time, color got bluer about 0.18 mag in r-i and 0.1 mag in i-z. R-I color also got bluer by 0.18 mag, and from the reddest point, it differed 0.25 mag.

We divide outburst stages of HBC 722 until 2013 May into five phases according to its brightness and color changes (see Table 3 and Figure 2). First, Phase 1 deals from the beginning of the outburst to the first brightness peak in 2010 September. The brightness rapidly increased and color got bluer in Phase 1. The following Phase 2 is from the first brightness peak to 2011 February during which the brightness got fainter and color became redder. These two phases are well presented in Semkov et al. (2010) and Miller et al. (2011). After dimming by 1.4 magnitude (R) during 6 months, the source remained relatively constant in brightness for another few months with only some small bounces, but color continuously got redder. We label it as Phase 3, which describes relatively constant state in the period of outburst. On the other hand, in Phase 4, from 2011 October, HBC 722 started to re-brighten slowly. It steadily recovered its luminosity and the color curves showed distinctive bluer tendency again until 2012 May. Lastly, in Phase 5, the brightness continuously increased and went over its first peak of luminosity in 2013 May observation. In contrast to Phase 4, color curves of the last phase have weak bluer tendency or close to remain constant with small fluctuations. According to Semkov et al. (2014), HBC 722 maintains similar brightness from the secondary peak in 2013 May.

Table 3: Classification of Phases

Period	JD (+2450000)	Description	Magnitude	Color
Phase 1	– 5460	Pre 1st Peak Increase	Brighter	Bluer
Phase 2	5461 – 5600	Post 1st Peak Decrease	Fainter	Redder
Phase 3	5601 – 5850	Post 1st Peak Constant	Constant	Redder
Phase 4	5851 – 6050	Pre 2nd Peak Fast Increase	Brighter	Bluer
Phase 5	6051 –	Pre 2nd Peak Slow Increase	Brighter	Constant

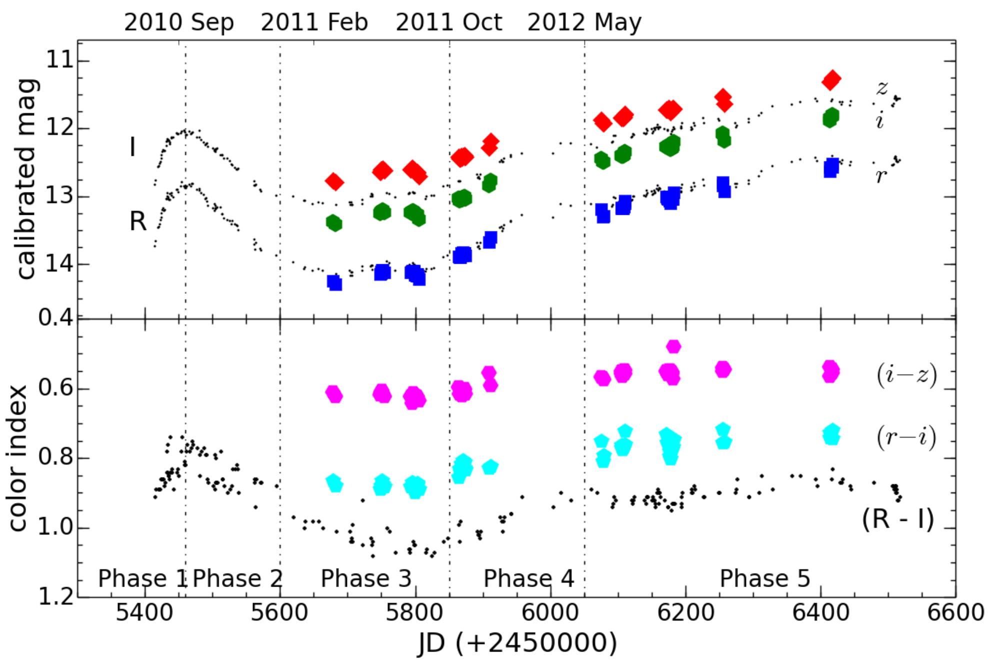

Fig. 2: Top: Light curve of HBC 722 collected during our observed period (2011 April – 2013 May). The upper (red), middle (green) and the the lower (blue) symbols represent light curves of z, i and r bands, respectively. For comparison, Semkov et al. (2012a, 2014) of I and R bands are also ploted in light green and light blue. Bottom: Color variations. The upper (pink) and middle (cyan) dotted curves represent i-z and r-i color indices respectively. We also plot the R-I color from Semkov et al. (2012a, 2014) as references (light brown). The small offsets between our data and references are from the different filter system.

We found hints of short term phenomena distinguished from the long term behaviors. Figure 3 shows sample data collected over two weeks in 2011 August. We averaged the data of each night to see day scale brightness and color variabilities. With respect to the long term, this period belongs to Phase 3 that HBC 722 stayed relatively constant in brightness and became redder in color (see Figure 2). However, with regard to the short term in Figure 3, day scale fluctuations are seen with the other short scale decreasing tendency of 0.1 mag amplitude. Besides, color hardly changed at the same time. This distinguished behaviors on different timescales imply that there could be shorter timescale mechanisms in HBC 722 system.

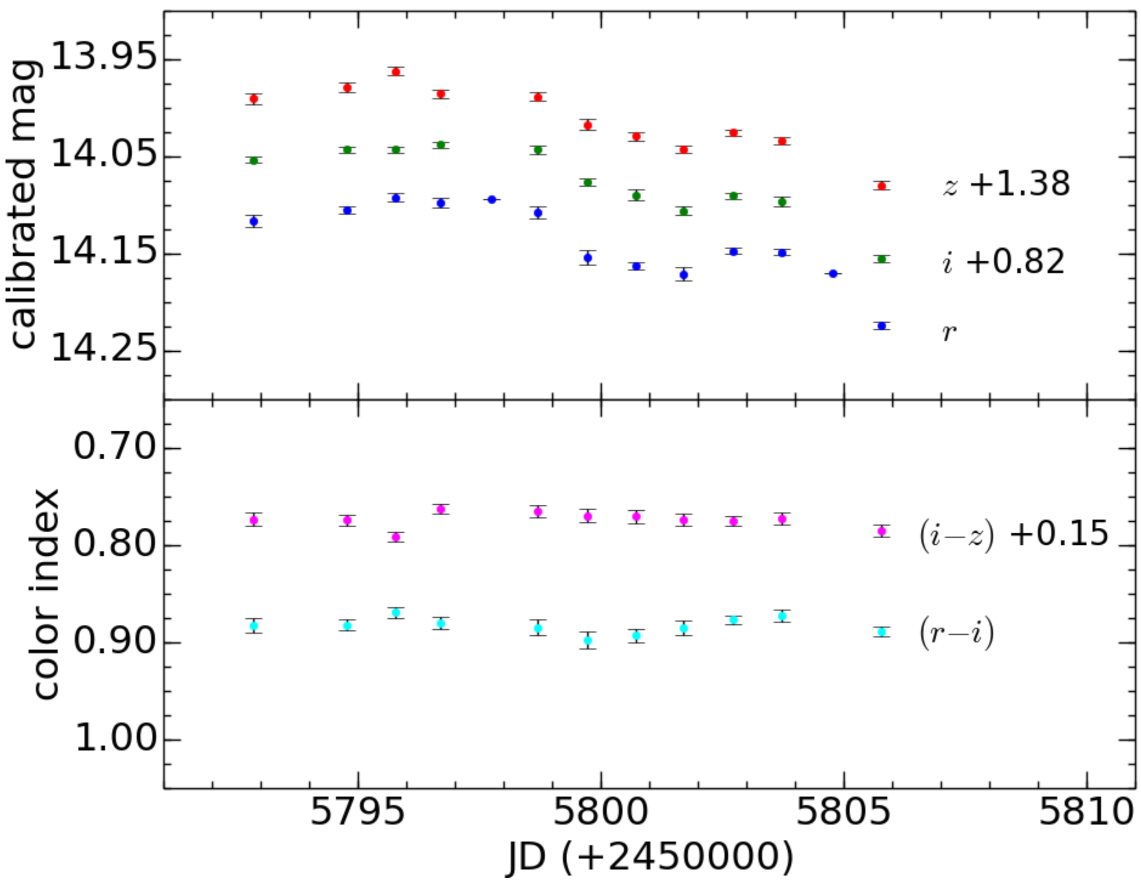

Fig. 3: Top: Sample of a day scale light curve over two weeks in 2011 August (Phase 3). The upper (red), middle (green) and the lower (blue) dots illustrate light curves of z, i and r bands, respectively. Data taken in a single night are averaged. For better visibility, offsets of +0.82 and +1.38 mag are applied to i and z bands, respectively. The light curve suggests the presence of day scale variabilities. Bottom: Color variations during the same period. The upper (pink) and the lower (cyan) dots represent i-z and r-i color respectively, averaged in a single night. The offset of 0.15 mag is applied to i-z color to check variation. During the same period, color hardly changed in the day scale.

3.2 Color-magnitude diagram

Based on our r, i and z bands photometry in Phase 3, 4, and 5, we present i vs. r-i and i-z color-magnitude diagram in Figure 4. The upper and lower layers depict i-z and r-i, respectively. Each point is obtained by averaging the whole data taken in a night. During overall observed period, both r-i and i-z colors have become bluer as brightness has increased. The r-i tendency is slightly steeper than i-z's. This is an expected behavior due to the temperature change of the source. When accretion-related variability occurs, the amount of energy from the source and emission distribution with wavelengths change. This phenomenon results in the variation of SED shape. At that time, the wavelengths range shorter than emission peak would lie on the blue edge or "Wien side" of SED, and thus this part is very sensitive to the temperature change (e.g., Hartmann 2008). In the case of HBC 722, the characteristic wavelengths are located at optical/near-infrared. Thus over the long term, the bluer tendency at optical/near-infrared colors as brightness increases is well understandable. We also analyze the data during each phase. Color remained constant in Phase 3 and got bluer when it entered to Phase 4. In Phase 5, i-z color remains almost constant again but r-i gets still bluer. Additionally, there are local fluctuations of a few days in the phases. In the long term, the grouped phases well follow the bluer trend, but in the short term, the order of a few days variation are fluctuating within the grouped phases, which is not in regular sequence along with the long term trend.

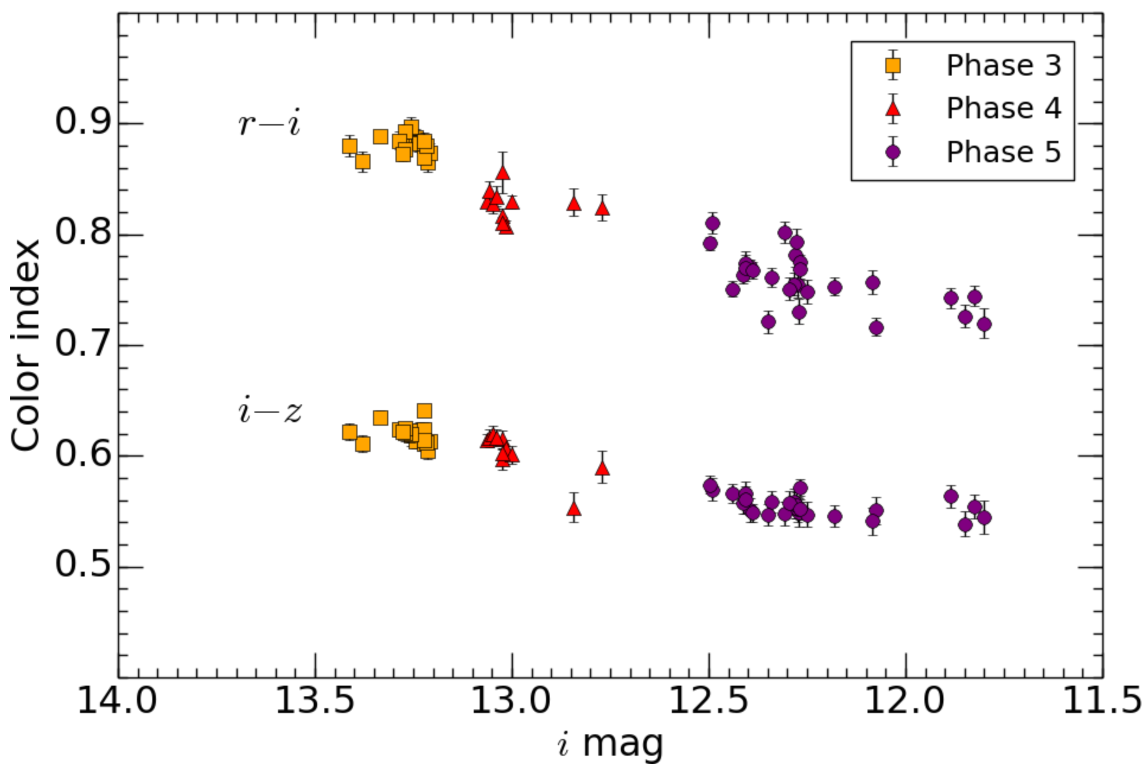

Fig. 4: Color-magnitude diagram during observed period. The upper and lower layers show i-z and r-i color indices respectively. To look at day scale color variation, the entirety of the data taken in a night are averaged.

3.3 Color-color diagram

Figure 5 shows r-i vs. i-z color-color diagram of our observation data. Points averaged over a single night are presented to see day scale behaviors. Again, data are grouped according to the phases. We hardly see color variations during Phase 3, but they moved toward a bluer direction with an increase in brightness in Phase 4. It remained in similar positions from Phase 5, in which the color hardly varied in i-z but got bluer in r-i. Both Figure 4 and 5 illustrate varying color features of HBC 722 in regard to the phases. Therefore, we argue that this color changes might be caused by altering physical properties in individual phases.

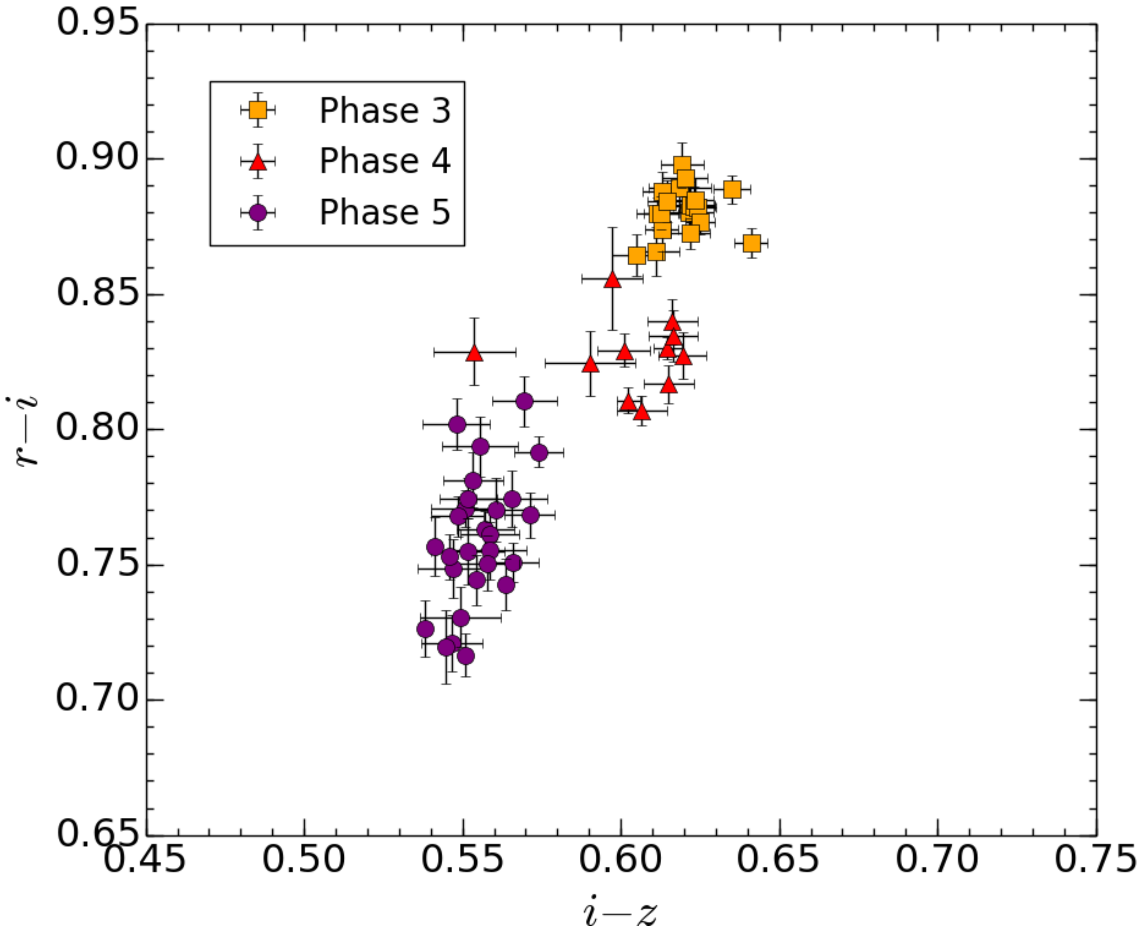

Fig. 5: Color-color diagram for observed period. Each dots represents the averaged data for a single night. We can find that the color hardly moved during Phase 3 (2011 February – 2011 August) and start to get bluer while the source brighten in Phase 4 and return to constant or less bluer status in Phase 5.

Chapter 4

Discussions

4.1 Spectral energy distribution (SED)

To look at the deviations of spectral emissions in the post-outburst phase, we plot the multiple SEDs for several different brightness states in Figure 6. We take Semkov et al. (2012b, 2014) for B, V, R, and I bands from the 2010 outburst to 2013 May. Data in r, i and z bands are taken from this work. For near-infrared, we take J, H and K_S band data from Kóspál et al. (2011), Antoniucci et al. (2013) and Sung et al. (2013). All literature data are converted from Vega magnitude to AB magnitude system by using Blanton & Roweis (2007). We match the archival data to our r, i and z data to construct SED with closest nights. The first SED is from the first peak in 2010, on the boundary between Phase 1 and Phase 2 in our criteria. We only use literature data taken in 2010 September 19 and 20. Second one represents Phase 3 which shows relatively calm state constructed by 2011 April 28, 30 and May 2. Third one is on the boundary between Phase 3 and Phase 4, when HBC 722 started to re-brighten. We use 2011 October 30 for all wavelengths data. Fourth one is on the boundary between Phase 4 and Phase 5, when it reached to similar brightness with the first peak brightness in 2010. We use 2012 May 20 and 27 for this state. The last one is from Phase 5 when it brighten up more than the first peak. We use 2013 April 14 May 4, 5.

To begin with, there is a main difference between the SED of re-brighten period and that of the first peak. The shape of SED for re-brighten period shows redder feature than that of first peak, even at Phase 5, when the brightness got over the first peak. Therefore comparing to the original flaring, HBC 722 showed more increase in brightness but less bluer in color at re-brightened period.

From Phase 3 to Phase 5, the shape of SED also changed slightly. The gradient becomes less steeper as HBC 722 got re-brightened up, which suggests the emission from shorter wavelength becomes higher. Thus in the long term, the source got bluer. It is well matched with our color analysis in previous section again. Johnstone et al. (2013) proved the time evolution of SED in outburst with their established model. When the accretion rate increases, the peak of SED moves toward a shorter wavelength which fits for a higher temperature blackbody. Also, they predicted that the first indication of heating is luminosity rise of the source at near or shorter wavelength region than the peak of SED. Our time evolution of SED in the re-brightened period shows a good agreement with their prediction.

Assuming that the emissions entirely came from disk accretion, we calculate relative accretion rate as a function of time. The bolometric luminosities limited at optical–near infrared are obtained in each phase (the same epochs with in SEDs). By taking accretion luminosity formula and properties of HBC 722 used in Green et al. (2013), accretion rates were driven. We normalize the values for the minimum brightness epoch of Phase 3 (2011 April) and present relative accretion rate change (Figure 7). The actual accretion rate obtained at the similar epoch to Phase 3 reported in Green et al. (2013) is $\dot{M} = 1.31\times10^{-6}$ $M_\odot$ yr^{-1}.

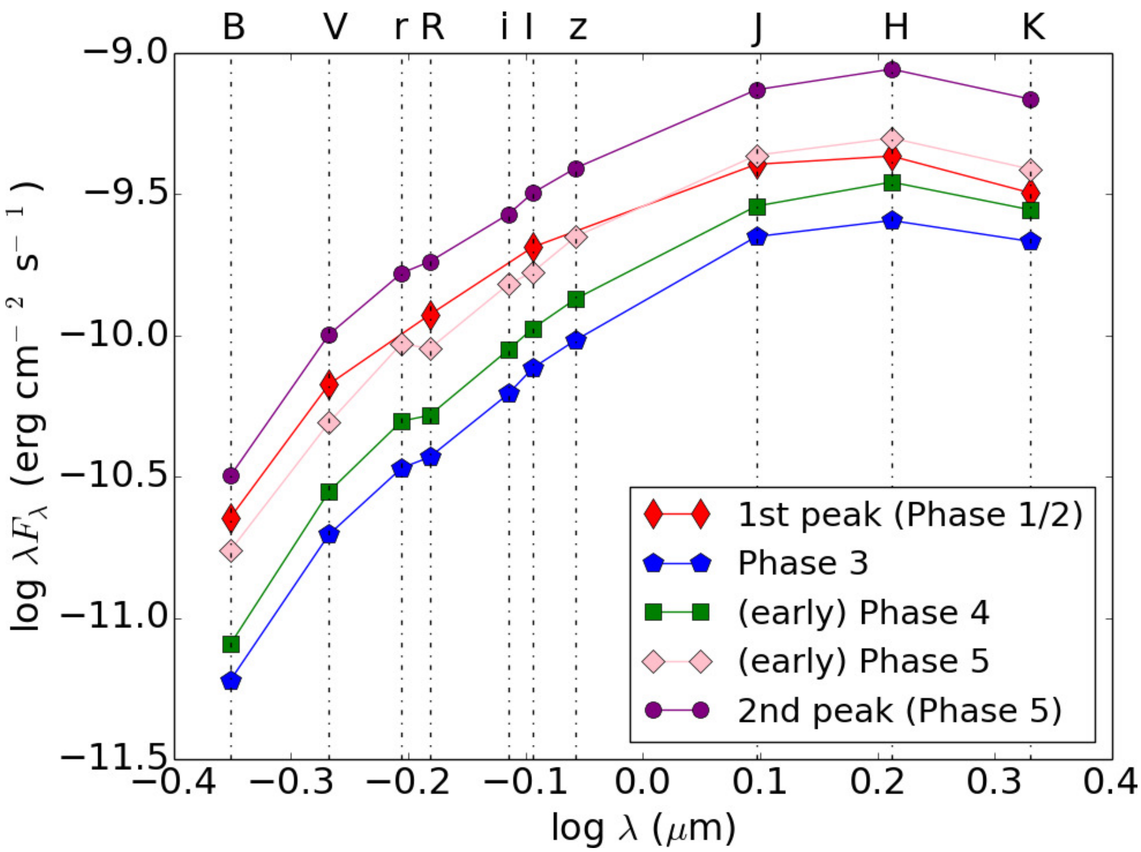

Fig. 6: Multi-epoch SEDs of HBC 722 after outburst. B, V, R, and I bands are from Semkov et al. (2012b, 2014). r, i and z bands are taken from this work. J, H and K_S data are taken from Kóspál et al. (2011), Antoniucci et al. (2013) and Sung et al. (2013). All data except r, i and z are converted from Vega to AB magnitudes system using Blanton & Roweis (2007).

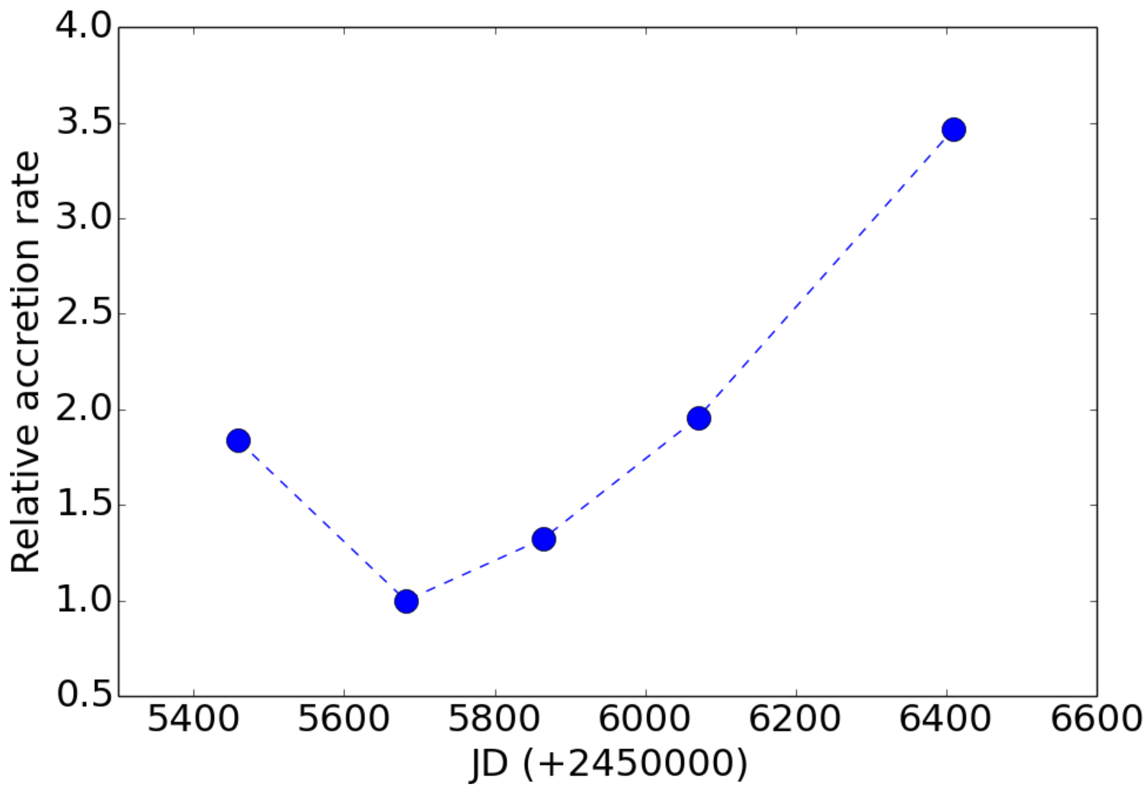

Fig. 7: Relative accretion rate at each phase. We normalize derived accretion rate values to the minimum brightness epoch after outburst (2011 April) to compare the change of accretion rate in the post outburst phase.

4.2 Flickering

Although only small number of outbursting YSOs have been detected, these uniquely enhanced systems provide how accretion process occurs from innermost part of circumstellar disk to central star, which play an important role for understanding the evolution of YSOs.

In accordance with Kenyon et al. (2000, and references therein.), "flickering" is randomly fluctuated small amplitude (0.01–1.0 mag) variations in dynamic timescales. It could be observed in cataclysmic variables and erupting YSOs. Flickering is often thought to be a signature of disk accretion. The most widely accepted origin of flickering is a temperature region between the central star and disk, which is the vicinity of inner edge of the disk. Since a large amount of disk material falls to the stellar surface from the inner disk, flickering could be evidence for inhomogeneous accretion flow (e.g., Shu et al. 1994; Bastien et al. 2011).

In order to check short term behaviors of intra-day and day time scales, we quantify the potential variabilities in r, i and z bands. We expect to see footprints of flickering by using a micro-variability method developed by Jang & Miller (1997).

$$C_1 = \frac{\sigma\,(Object - Comp1)}{\sigma\,(Comp1 - Comp2)} \quad and \quad C_2 = \frac{\sigma\,(Object - Comp2)}{\sigma\,(Comp1 - Comp2)} \tag{4.1}$$

C_1 is calculated by standard deviation of differential photometry for an object (Object) and a comparison star (Comp1) divided by that of the comparison star (Comp1) and a check star (Comp2). C_2 is also calculated in the same manner. Finally we derived the parameter (C) by taking the average of C_1 and C_2 (e.g., Romero et al. 1999; Gupta et al. 2008). According to Jang & Miller (1997), parameter C depends on normal distribution, so we can suggest that potential variabilities exist with 90%, 95% and 99% confidence level with C values of 1.64, 1.96 and 2.57, respectively. Therefore, we substitute HBC 722, C7 and C4 for Object, Comp1 and Comp2, respectively.

The result of day scale variability of HBC 722 can be found in Table 4 and Figure 8.

We do not include 2011 April, 2011 December, 2012 May and 2012 November runs because each covered only a few nights including not photometric nights. For the majority of nights, C values are over 2.57, which implies HBC 722 has variability with a 99% confidence level in the day scale. On the other hand, C_r in 2011 July, C_r and C_i in 2011 November and C_i in 2012 September have values between 1.96 and 2.57. According to the aforementioned rule, these have 95% confidence for their variabilities. Lastly, C_z in 2011 July is located between 1.64 and 1.96, which is a little less confident than the others, but we still have 90% confidence of variability. To sum up, HBC 722 strongly shows day scale variability in 2011 August, 2012 June and 2013 May. It displays meaningful variabilities in the other months as well. Therefore, we conclude that HBC 722 is flickering. Since there is no certain relation between the length of observation and amplitude of brightness change, it is unlikely that the duration of continuous observation affects the C values.

According to the historical efforts to find clues of flickering in the outburst stage of cataclysmic YSOs, many studies focused on finding day scale periodic and aperiodic variations. However, using the properties of low mass YSOs and their Keplerian disks, we can explore IDV, which could exist between the innermost part of the disk and the central star. Opportunely, our observing time at the re-brightened status of HBC 722 is related to the re-stimulated disk accretion activity. Because of our short cadence monitoring observation strategy, we can also look at the behaviors of HBC 722 in intra day scale. We quantify the IDV in the same manner with the day scale variability. The results of derived C values are tabulated in Table 5.

Table 4: Result of day scale variability of HBC 722.

Month	Filter	Duration [Day]	C_r	C_i	C_z
2011-07	r,i,z	6	2.54	2.73	1.83
2011-08	r,i,z	13	4.86	6.63	4.69
2011-11	r,i,z	9	2.44	2.42	1.59
2012-06	r,i,z	7	4.97	4.34	3.29
2012-09	r,i,z	11	2.68	1.98	1.42
2013-05	r,i,z	4	3.39	3.93	2.83

Note. – C values represent relative brightness derivation to that of comparison star. It provide statistical confidences of variability of the source. C value above 1.64, 1.96 and 2.57 infer confidence level of the variability in 90%, 95% and 99% respectively.

In analysis of micro-variability of each night, we observed a point on 2012 September 6 to have a z band over 2.57, suggesting variability with a 99% confidence level. C_r and C_i on 2011 July 5, C_i on 2012 September 2 and 2013 May 1 have between 1.96 and 2.57, which means potential variabilities with a 90% confidence level. Additionally, C_r on 2011 August 24, 2011 November 4, 2012 September 6 and 2013 May 5 are all between 1.64 and 1.96, which implies a 90% of potential variability. Meanwhile, many of the C values in z band, and a few of r and i bands, are lower than 1.0. Since the micro-variability method depends on the comparison and check star, these values can be caused by the brightness differences among the object (HBC 722), comparison (C7) and check stars (C4). In this analysis, IDV is less convincing than day scale variability. Note that we suggest statistical values for variability rather than specific values.

There are several previous studies of short term variability of FUors. Herbig (2003) observed FU Orionis and revealed $\sim$14 days of spectroscopic periodicity in P Cygni profiles, especially in Hα, lasting more than 1.5 years. The author also discovered another 3.54 days of periodic variation arising from inner structure of photosphere. Powell et al. (2012) confirmed the periodicities found by Herbig (2003) and suggested that the periodic phenomena continued over 10 years. Recently Siwak et al. (2013) discovered 2–9 day quasi-periodic features in FU Orionis using the Microvariability and Oscillations of STars ($MOST$) satellite. Furthermore, Siwak et al. (2013) stated that it could be caused by a dump of plasma, or magneto-rotationally unstable heterogeneities in the localized accretion disk rotating at different Keplerian radii. Meanwhile, Clarke et al. (2005) reported day scale non-periodic fluctuations in another classical FUors. They detected photometric variabilities with amplitudes of 0.1 and 0.3 mag (V) for V1057 Cyg and V1515 Cyg, respectively, which might be caused by flickering events.

Table 5: Result of intra-day variability (IDV) of HBC 722.

Date (UT)	Filter	Number of frames	Observing time [hour]	C_r	C_i	C_z
2011-04-26	r,i,z	24	0.5	1.10	0.80	1.19
2011-07-05	r,i,z	311	4.5	2.11	2.04	1.48
2011-07-11	r,i,z	47	0.9	1.16	1.47	1.04
2011-08-24	r	1125	7.5	1.68	···	···
2011-08-31	r	791	5.7	1.43	···	···
2011-11-02	r,i,z	211	5.3	1.50	1.08	0.82
2011-11-04	r,i,z	116	2.9	1.71	1.24	0.98
2011-11-09	r,i,z	206	4.9	1.50	1.32	1.06
2012-05-27	r,i,z	128	2.7	0.90	1.24	0.82
2012-05-30	r,i,z	300	3.8	1.45	0.96	0.90
2012-06-28	r,i,z	399	6.2	1.42	0.88	0.96
2012-07-01	r,i,z	182	4.0	1.45	1.05	0.88
2012-07-02	r,i,z	32	0.5	1.06	1.24	0.94
2012-09-01	r,i,z	328	6.2	1.07	1.22	1.18
2012-09-02	r,i,z	492	7.1	0.97	2.29	1.01
2012-09-03	r,i,z	219	5.2	1.03	1.39	0.87
2012-09-06	r,i,z	23	0.5	1.98	1.89	2.95
2012-09-07	r,i,z	31	0.5	1.19	0.98	0.82
2012-09-09	r,i,z	177	6.3	1.24	1.52	0.92
2012-11-26	r,i,z	53	0.5	0.93	1.06	1.00
2013-04-30	r,i,z	162	2.2	0.99	1.10	0.86
2013-05-01	r,i,z	144	1.7	1.24	2.20	0.98
2013-05-04	r,i,z	143	2.2	0.99	1.03	0.80
2013-05-05	r,i,z	150	1.8	1.68	1.70	0.76

Note. – C values for the confidence level follow the same rule in Table 4.

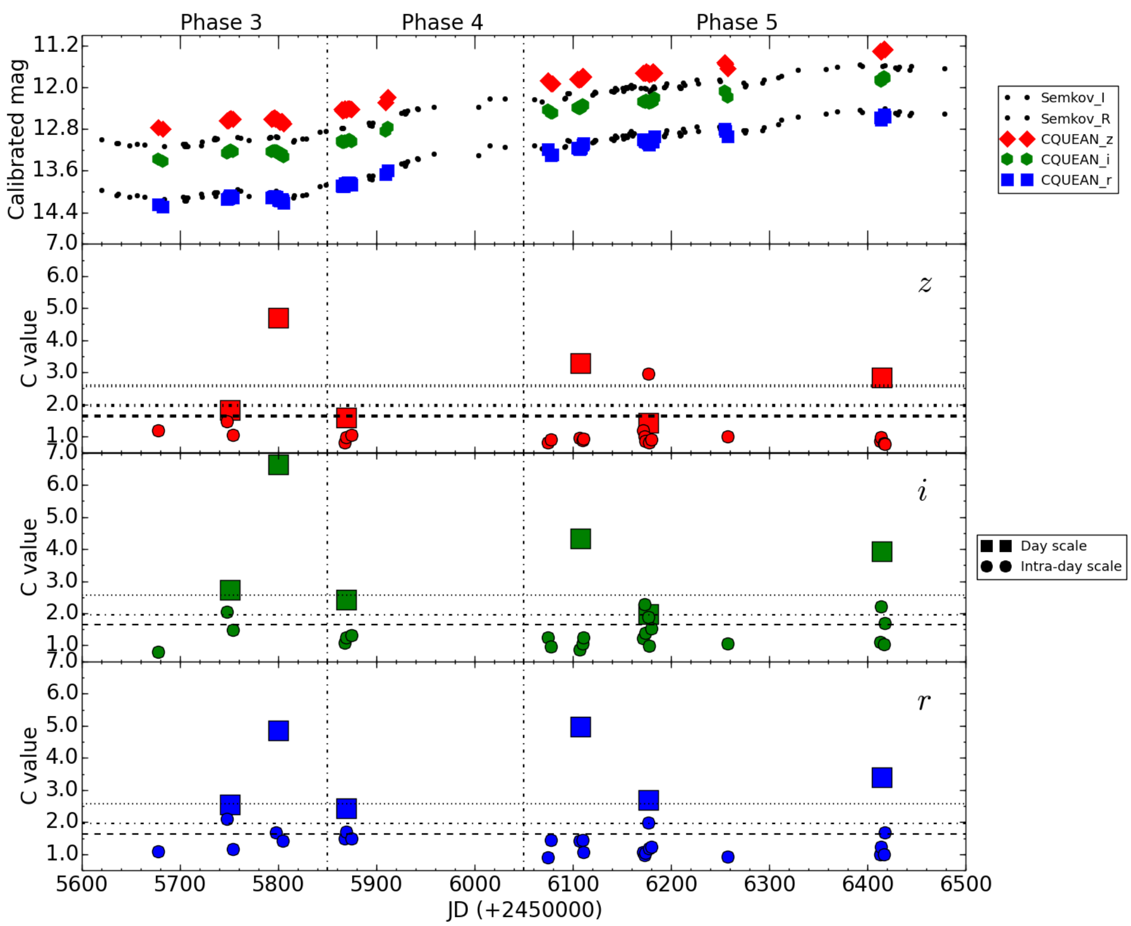

Fig. 8: Overall light curves and plots of C values. The top plot shows light curves from 2011 April to 2013 May as a reference for long term brightness variation. The upper (red), middle (green) and lower (blue) plots show z, i and r bands. From the second to the fourth show C values distribution for z, i and r band, respectively. Large squares and small circles indicate day scale from Table 4 and intra-day scale from Table 5, respectively.

In HBC 722, day scale non-periodic variabilities are detected similar to the V1057 Cyg and V1515 Cyg cases. Because two classical FUors are brighter than HBC 722 in optical, it is plausible that HBC 722 is flickering with smaller amplitude. We found the variabilities last more than 2 years with diverse amplitudes.

Looking back to other studies of IDV for flaring YSOs, Kenyon et al. (2000) collected photometric data of FU Orionis and detected random brightness fluctuations in a dynamic timescale of a day or less, with 0.035–0.1 mag amplitude (V). Bastien et al. (2011) conducted rapid cadence time series photometry for V1647 Orionis in the outburst stage, which belongs to another eruptive YSO, EXors. As a result, 0.13 day (51 mmag amplitude) periodic variability was found. They believed that the periodic variability would be related to flickering by detecting 'flickering noise' signs in the power spectrum of the light curves. Since HBC 722 still remains enhanced, further investigation with sufficient data will more clearly reveal IDV and properties of intra-day flickering.

In Figure 8, we attempt to find a relation between long term brightness change and short term variability. Two of the C values around 2011 August and 2012 September are particularly large, and they lie at the boundary between the phase lines (noted in Table 3). These larger points near the boundary of phases might be interpreted as a result of a transition to the next phases as one of possible interpretation. It can be proved if additional short term variabilities are detected when the long term brightness tendency changes. Finally, we find a tentative relation that C values get lower from r to z, implying smaller amplitude of variation in longer wavelength. A few explanations might be possible: first, this tendency can be simply due to the brightness effect. Under assumption of no intrinsic variabilities for two objects, brighter star shows smaller brightness deviation than dimmer one. In our case, HBC 722 clearly shows intrinsic variability but this brightness effect would be added. In r, i and z bands HBC 722 is brighter than comparison stars but the brightness difference in z band is greater than that in r band. Since C values that we used is obtained by relative amount of brightness deviation from that of comparisons, the values could be affected by brightness difference in each band. Therefore the C values could decrease with increasing wavelengths. Second, intrinsic characteristics of HBC 722 could appear. Sung et al. (2013) reported that HBC 722 showed strong correlation between flux variation and fading period after outburst. They estimated the flux variation from maximum brightness in 2010 to minimum in 2011 and compared it with fading period. As a result, both flux variation and fading timescale are larger at shorter wavelengths. The flux variation tends to decrease linearly as wavelength increases in the optical/near-infrared range. Therefore we could expect that there is an inverse proportion relation between wavelengths (r, i and z bands) and amplitudes.

Chapter 5

Conclusion

We observed HBC 722 in SDSS r, i and z bands from 2011 April to 2013 May with CQUEAN attached to the 2.1m Otto Struve telescope at McDonald Observatory. The photometric results show that HBC 722 have re-brightened for 2 years and presented unprecedented high brightness. The color also have become bluer at the same period. However, the brightness and color occasionally maintained similar status rather than steadily changed, which could be related to physical processes in inner disk. Thus we divided the post-outburst phase into five according to brightness and color variations. We analyze color-magnitude diagram and color-color diagram to depict tendency along with the phases and possible day scale variabilities. Different shapes of optical/near-infrared emissions between at the first peak and henceforward are shown in spectral energy distribution. Additionally, multi-epoch SED shapes indicate that HBC 722 has become hotter as brightness have increased.

We also investigate short term variability separated from long term variations to find indications of flickering. By using micro-variability method, intra-day and day scale variability are quantified. We find clear evidences of day scale variabilities and weaker signs of IDV for r, i and z bands. Comparing these short term variabilities with long term brightness variations in Phase 3 to Phase 5, derived C values of variabilities tend to display larger number on nearly boundary of phases. We suggest that there could be transitions of physical processes at the innermost part of disk which attribute to the change of brightness and color behaviors.

Bibliography

Audard, M., Ábrahám, P., Dunham, M., M. et al. 2014, review chapter in Protostars and Planets VI, University of Arizona Press (2014), eds. H. Beuther, R. Klessen, C. Dullemond, Th. Henning, 1401, 3368, in press

Antoniucci, S., Arkharov, A., Klimanov, S., et al. 2013, ATel, 5023,1

Bastien, F. A., Stassun, K. G., Weintraub, D. A. 2011, AJ, 142, 141

Bell, K. R., & Lin, D. N. C. 1994, ApJ, 427, 987

Bertin, E., & Arnouts, S. 1996, A&AS, 117, 393

Blanton, M. R., & Roweis, S. 2007, AJ, 133, 734

Clarke, C., Lodato, G., Melnikov, S. Y., Ibrahimov., M., A. 2005, MNRAS, 361, 942

Cohen, M., & Kuhi, L. V. 1979, ApJS, 41, 743

Fukugita, M., Ichikawa, T., Gunn, J. E., et al. 1996, AJ, 111, 1748

Goodrich, R. W. 1987, PASP, 99, 116

Green, J. D., Robertson, P., Baek, G., et al. 2013, ApJ, 764, 22

Gupta, A. C., Cha, S.-M., Lee, S., et al. 2008, AJ, 136, 2359

Hartmann, L., & Kenyon, S. J. 1996, ARA&A, 34, 207

Hartmann, L. 2008, Accretion Processes in Star Formation Second Edition, (Cambridge astrophysics series, 47; Cambridge: Cambridge Univ. Press)

Herbig, G. H., Petrov, P. P., Duemmler, R. 2003, ApJ, 595, 384

Johnstone, D., Hendricks, B., Herczeg, G., Bruderer, S. 2013, ApJ, 765,133

Kim, E., Park, W.-K., Jeong, H., et al. 2011, JKAS, 44, 115

Kenyon, S. J., Kolotilov, E. A., Ibragimov, M. A., Mattei, J., A. 2000, ApJ, 531, 1028

Kóspál, Á., Ábrahám, P., Acosta-Pulido, J. A. et al. 2011, A&A, 527, 133

Lim, J., Chang, S., Pak, S., et al., 2013, JKAS, 46, 161

Lee, J.-E., Kang, W., Lee, S.-G., et al. 2011, JKAS, 44, 67

Laugalys, V., Straižys, V., Vrba, F. J., et al., 2006, Baltic Astronomy, 15, 483

Miller, A. A., Hillenbrand, L. A., Covey, K. R., et al. 2011, ApJ, 730, 80

Jang, M., Miller, H. R. 1997, AJ, 114, 565

Park, W.-K., Pak, S., Im, M., et al. 2012, PASP, 124, 839

Powell, S. L., Irwin, M., Bouvier, J., Clarke, C., J. 2012, MNRAS, 426, 3315

Romero, G. E., Cellone, S. A., Combi, J. A. 1999, A&AS, 135, 477

Semkov, E. H., Peneva, S. P., Munari, U., et al. 2010, A&A, 523, 3

Semkov, E. H., Peneva, S. P., Munari, U., et al. 2012a, yCat, 354, 29043

Semkov, E. H., Peneva, S. P., Munari, U., et al. 2012b, A&A, 542, 43

Semkov, E. H., Peneva, S. P., Ibryamov, S., I., Dimitrov, D., P. 2014, BlgAJ, 20, 59

Shu, F., Najita, J., Ostriker, E., et al. 1994, ApJ, 429, 781

Siwak, M., Rucinski, S. M. Matthews, J. M., et al. MNRAS, 432, 194

Skrutskie, M. F., Cutri, R. M., Stiening, R., et al. 2006, AJ, 131, 1163

Smith, J., A., Tucker, D. L., Kent, S., et al. 2002, AJ, 123, 2121.

Sung, H.-I., Park, W.-K., Yang, Y., et al. 2013, JKAS, 46, 253.

Weintraub, D. A., Sandell, G., Duncan, W. D. 1991, ApJ, 382, 270

Wright, E., L., Eisenhardt, P., R., M., Mainzer, A., K., et al. 2010, AJ, 140, 1868